

# BEST INDIVIDUAL TEMPLATE SELECTION FROM DEFORMATION TENSOR MINIMIZATION

Natasha Lepore<sup>1</sup>, Caroline Brun<sup>1</sup>, Yi-Yu Chou<sup>1</sup>, Agatha D. Lee<sup>1</sup>, Marina Barysheva<sup>1</sup>,  
Xavier Pennec<sup>2</sup>, Katie L. McMahon<sup>3</sup>, Matthew Meredith<sup>3</sup>, Greig I. de Zubicaray<sup>3</sup>,  
Margaret J. Wright<sup>4</sup>, Arthur W. Toga<sup>1</sup>, Paul M. Thompson<sup>1</sup>

<sup>1</sup> Laboratory of Neuro Imaging, Department of Neurology, UCLA School of Medicine, Los Angeles, CA 90095, USA

<sup>2</sup> INRIA Sophia - Asclepios Project, Sophia Antipolis, France

<sup>3</sup> Centre for Magnetic Resonance, University of Queensland, Brisbane, Australia

<sup>4</sup> Genetic Epidemiology Lab, Queensland Institute of Medical Research, Australia

## ABSTRACT

We study the influence of the choice of template in tensor-based morphometry. Using 3D brain MR images from 10 monozygotic twin pairs, we defined a tensor-based distance in the log-Euclidean framework [1] between each image pair in the study. Relative to this metric, twin pairs were found to be closer to each other on average than random pairings, consistent with evidence that brain structure is under strong genetic control. We also computed the intraclass correlation and associated permutation  $p$ -value at each voxel for the determinant of the Jacobian matrix of the transformation. The cumulative distribution function (cdf) of the  $p$ -values was found at each voxel for each of the templates and compared to the null distribution. Surprisingly, there was very little difference between CDFs of statistics computed from analyses using different templates. As the brain with least log-Euclidean deformation cost, the mean template defined here avoids the blurring caused by creating a synthetic image from a population, and when selected from a large population, avoids bias by being geometrically centered, in a metric that is sensitive enough to anatomical similarity that it can even detect genetic affinity among anatomies.

**Index Terms**— brain, image analysis, Magnetic Resonance Imaging

## 1. INTRODUCTION

The choice of a common template space is essential for many analyses comparing or integrating neuroanatomical data across subjects. Among these methods, tensor-based morphometry (TBM) computes local statistical differences in brain anatomy between groups of subjects, based on deformations that align scans to a common template. A set of MR images is nonlinearly registered to a reference image, either

from one of the individual subjects [12] or an average image computed from a subset of the data [13, 17]. The Jacobian matrices  $J$  resulting from the deformation are computed and statistically analyzed to obtain a map of group differences at each voxel, or of the effects of covariates on anatomy (e.g., age or genetic risk for disease).

In the most commonly used version of TBM [22, 2], statistics at each voxel are computed from the determinant of the Jacobian matrix, which stores information on regional differences in volumes of brain substructures. However, in [16], we showed that multivariate statistics on the deformation (or strain) tensors

$$S = \sqrt{J^T J} \quad (1)$$

outperformed this scalar measure for detecting morphometric brain differences between HIV/AIDS patients and healthy controls. As the statistics were computed on the deformation tensors, a mean template was designed in [17] that defined the average deformation as the mean of the deformation tensors at each voxel, computed in the log-Euclidean framework [1]. The control brain already closest to the average was moved by gradient descent in the direction of this average. In a 2D analysis of the corpus callosum in HIV/AIDS patients, the average template constructed in this way did not differ in detection power (measured by effect sizes in TBM) when compared to that of using a single individual brain as template.

Construction of a mean anatomical template, in a strictly defined mathematical sense, may reduce the bias induced by registering images to an individual control subject. Even so, the features and anatomical boundaries are typically sharper in individual brain images, so using them as a template may allow for a more accurate registration, which may in turn improve detection power in a study of registration mappings. In [6], the template from an individual control outperformed the average ICBM53 atlas brain as a registration target image for TBM, in the sense that more widespread atrophy was detected in HIV/AIDS, with greater effect sizes at each voxel. In most

This work has been partly supported by the Brain-Atlas grant from INRIA's "Associate Team" program

studies, the individual brain is usually selected by visual inspection as one that is visually representative of the sample. However, few studies to date have selected individual brains based on mathematical criteria or examined the influence of the chosen target brain on the statistical results.

As our statistics are computed from the deformation tensors at each voxel, one potential template optimization strategy is to choose an individual brain which is already the most average among the subjects, with respect to a metric. This approach is similar in philosophy to that used in [13], where an optimized template was selected as the brain closest to the average of the deformation fields. Here, we instead define the total distance between the image set and the template image  $i$ , denoted  $E_i$ , as the distance  $d(.,.)$  to all the deformation tensors  $S_i$  generated through the transformation from  $i$  to all other images in the data set ( $Id$  denotes the identity):

$$E_i = \sum_i \int d(S_i, Id)^2 \quad (2)$$

As an application of this approach, we examine brain MRI data from twins. Twin data has been used to examine genetic influences on brain structure using TBM [15, 5], diffusion tensor imaging (DTI) [14], high angular resolution diffusion imaging (HARDI) [7] and using surface based analyses of cortical gray matter density [23, 24]. Here we selected 10 pairs of monozygotic twins (MZs), and examined the relationship between (1) the templates distance  $E_i$  to the rest of the sample, and (2) the final statistics. We used the voxel-wise intraclass correlation as a measure of resemblance between genetically identical twins, as this would be a statistic for which registration errors - which may depend upon the choice of registration target - may deplete the measured correlation, sacrificing statistical power. To avoid assuming a Normal distribution for the resulting Jacobian determinants,  $p$ -values were computed from a permutation distribution at each voxel [20].

## 2. DATA

Subjects included a total of 10 pairs of MZ twins (4 male pairs and 6 female pairs) scanned as part of a 5-year imaging study of 1150 twins. At the time of testing, the twins were 21-27 years old (mean age 23.8 years). All MR images were collected using a 4 Tesla Bruker Medspec whole body scanner (Bruker Medical, Ettingen, Germany) at the Center for Magnetic Resonance (University of Queensland, Australia). Three-dimensional T1-weighted images were acquired with an inversion recovery rapid gradient echo (MP-RAGE) sequence to resolve anatomy at high resolution. Acquisition parameters were as follows: inversion time (TI)/repetition time (TR)/echo time (TE) = 1500/2500/3.83 msec; flip angle = 15 degrees; slice thickness = 0.9 mm, with an acquisition matrix of 256 x 256 x 256. All images were first spatially normalized to the ICBM-53 standard brain imaging template [10] by

a 6-parameter (3 translations, 3 rotations) transformation.

## 3. METHOD

As the deformation tensors do not form a vector space under the usual operations of matrix addition and scalar multiplication, all computations were performed in the log-Euclidean framework [1]. The distance between two deformation tensors  $S_1$  and  $S_2$  is then given by

$$d(S_1, S_2) = \|\log S_1 - \log S_2\|,$$

where  $\|\cdot\|$  denotes a norm, and  $\log$  is the matrix logarithm. Following [1], we will use

$$d(S_1, S_2) = (\text{Trace}(\log S_1 - \log S_2)^2)^{1/2}. \quad (3)$$

Thus, taking into account Eq. 3, Eq. 2 becomes

$$E_i = \sum_i \int \|\log S_i\|^2 d^3x = \sum_i \int \text{Tr}(\log S_i^2) d^3x \quad (4)$$

To compute the displacement fields, we used a fluid registration algorithm [18, 9] with a summed-squared-difference intensity-based cost function. In this approach each brain image is driven into the shape of the template using a linearized Navier-Stokes flow, driven by a distributed internal force that causes the intensity similarity to be optimized. The registration was accelerated using a fast filter, based on the Green's function of the linear elasticity operator, first designed in [3].

## 4. RESULTS

In **Figure 1**, we show the distance  $E_{ij}$  from subject  $i$  to  $j$ , for each of the individuals in the study. In most cases, members of a twin pair fall close to each other when compared to their distances to other subjects. The brains of monozygotic twins are in fact anatomically more similar than those of random pairs of individuals [17], so our distance may provide a measure of anatomical resemblance, which is sensitive to genetically mediated similarities in brain structure. Total distances  $E_i$  for each subject  $i$  are shown in Table 1.

Next, we computed the voxelwise permutation  $p$ -values for the intraclass correlation, between twins, for regional brain volumes, as estimated from the Jacobian determinants of the deformation mappings. We repeated this analysis, using each subject in turn as a template. In **Figure 2**, we show the cumulative distribution function (cdf) for the  $p$ -values that we obtained. For samples from a null distribution, the cdf should fall, on average, on the  $x = y$  axis. Cdfs based on using each of the 20 subjects as a registration target are shown in Fig. 2a. In Fig. 2b, we compare the cdfs from a typical twin pair, and in Fig. 2c, those of the brains which have the smallest and largest values of  $E_i$ . The cdfs for the twins fall much closer to one another, as expected.

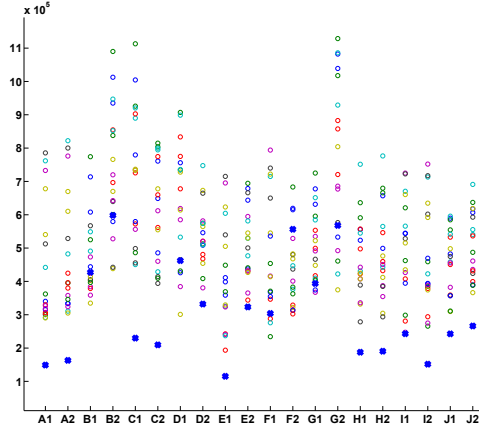


**Fig. 1.** Distance  $E_{ij}$  from each of the twins to all others. The  $x$ -axis labels the twin, and the  $y$ -axis its distance  $E_{ij}$  to each of the other twins (plotted as colored o's). The blue x in each column represents the distance to the second twin in the pair. In general, each subject is anatomically closer to their twin counterpart than to other randomly selected individuals from the sample, in line with the hypothesis that there are strong genetic influences on brain structure. Though the log-Euclidean distance is symmetric,  $E_{ij} \neq E_{ji}$  as the registration algorithm is not inverse-consistent, and furthermore, the distances are computed on masked templates, and thus depend on the brain size of each individual template.

## 5. DISCUSSION

This work is complementary to other efforts generating mean neuroanatomical templates for computational anatomy. Many efforts have focused on defining minimum mean-squared error (MMSE) anatomical templates in the sense that they deviate least from other anatomies in some intensity-based metric, or in some deformation norm (such as the LDDMM metric on the space of diffeomorphisms [19]), or a combination of both; even time-varying averages can be defined [11] as can cross-subject averages of multi-modality data, using information present in all modalities for registration.

Although these resulting templates are geometrically centered with respect to a metric, the resulting brain images typically do not retain sharp features, especially at the cortex, where the intensity averaging degrades cortical geometry to a great extent, no matter how well cortical anatomy is aligned. We therefore used tensor based deformation norms to select a candidate target brain, without resampling it or averaging it with other images to further minimize the norm. This approach does not require the computation of a new synthetic image as a registration target, but merely selects a representative image using a mathematically defined norm, retaining high-contrast features and boundaries that typically assist registration.

A good metric of anatomical difference should be sensi-

A1	0.8087	A2	0.8760
B1	0.9073	B2	1.3852
C1	1.3295	C2	1.1267
D1	1.1868	D2	1.0022
E1	0.7677	E2	0.9642
F1	0.8830	F2	0.8420
G1	0.9748	G2	1.4338
H1	0.8716	H2	0.8977
I1	0.9293	I2	0.8662
J1	0.8538	J2	0.9446

**Table 1.** Total distance  $E_i$  for each twin. The letter in each name represents the pair, and the number is the twin number, 1 or 2.

tive to the fact that twin brains resemble each other to a higher degree than random pairings. Thus, the twin design was used here to help establish that our proposed deformation metric, based on deformation tensors in a log-Euclidean space, is a valid measure of anatomical resemblance. In future, it would be interesting to establish further the heritability of  $E_{ij}$ , applying it to the search for genes that influence brain shape by fitting structural equation models, at each image voxel, to the maps of the energy density in each subject.

Ultimately the best template for optimizing multivariate statistics depends on the norm used in the statistical analysis, as well as the trade-off between computational efficiency, the complexity of the registration approach, and the power gained by improved registration relative to the power available with poorer (e.g., linear) registration. The results obtained here may be further improved by the use of a registration algorithm that explicitly regularizes the log-transformed deformation tensors, such as those found for instance in [5] and [21].

## 6. REFERENCES

- [1] Arsigny V et al., *Log-Euclidean metrics for fast and simple calculus on diffusion tensors*, Mag. Res. in Med. 56, (2006) 411–421.
- [2] Ashburner J, *A fast diffeomorphic image registration algorithm*, Neuroimage 38, (2007) 95–113.
- [3] Bro-Nielsen M, Gramkow C, *Fast fluid registration of medical images*, Vis. in Biomed. Comp., (1996) 267–276.
- [4] Brun C et al., *Comparison of Standard and Riemannian Elasticity for Tensor-Based Morphometry in HIV/AIDS*, MICCAI workshop on Statistical Registration: Pair-wise and Group-wise Alignment and Atlas Formation, (2007).
- [5] Brun C et al., *A new registration method based on log-Euclidean metrics and its application to genetic studies*, ISBI (2008).

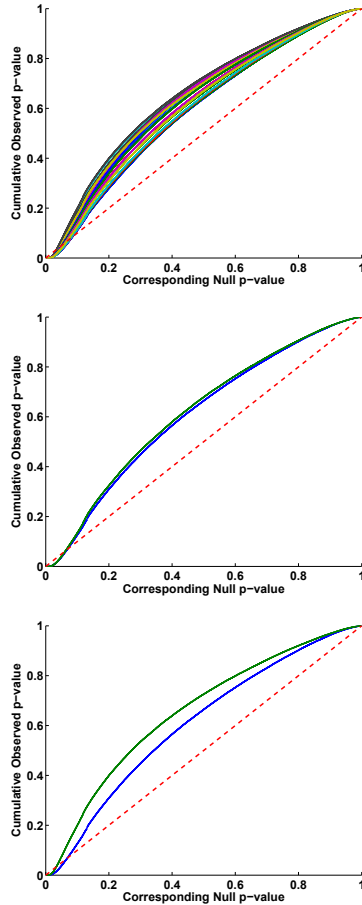


**Fig. 2.** Cumulative distribution of  $p$ -values for the voxelwise intra-class correlation *versus* the corresponding cumulative  $p$ -value that would be expected from a null distribution. Top: cdfs for all subjects in the study. Middle: cdfs for a typical twin pair. Bottom: cdfs for the brains with the highest (green) and lowest (blue) distances  $E_i$  to all the other brains in the study. Dotted line:  $x = y$  curve (null distribution). There is no significant difference between the “most average” and the “least average” templates in the study.

- [6] Chiang MC et al., *3D pattern of brain atrophy in HIV/AIDS visualized using tensor-based morphometry*, Neuroimage 34, (2007) 44–60.
- [7] Chiang MC et al., *Mapping Genetic Influences on Brain Fiber Architecture with High Angular Resolution Diffusion Imaging (HARDI)*, ISBI (2008).
- [8] Chou YY et al., *Quantitative genetic modeling of lateral ventricular shape and volume using multi-atlas fluid image alignment in twins*, ISBI (2008).
- [9] Christensen GE et al., *Deformable templates using large deformation kinematics*, IEEE-TIP 5, (1996) 1435–1447.
- [10] Collins DL et al., *Automatic 3D intersubject registration of MR volumetric data in standardized Talairach space*, JCAT 18: (1994) 192–205.
- [11] Davis BC et al., *Population Shape Regression From Random Design Data*, ICCV (2007).
- [12] Kochunov P et al., *An optimized individual target brain in the Talairach coordinate system*, Neuroimage 17, (2003) 922–927.
- [13] Kochunov P et al., *Regional spatial normalization: toward an optimal target*, JCAT 25, (2001) 805–816.
- [14] Lee AD et al., *Comparison of fractional and geodesic anisotropy in monozygotic and dizygotic twins from diffusion tensor imaging*, ISBI (2008).
- [15] Leporé N et al., *Genetic influences on brain structure and fiber architecture mapped using diffusion tensor imaging and Tensor-Based Morphometry in twins*, HBM (2006).
- [16] Leporé N et al., *Generalized Tensor-Based Morphometry of HIV/AIDS using multivariate statistics on deformation tensors*, IEEE-TMI 27, (2008) 129–141.
- [17] Leporé N et al., *Mean template for Tensor-Based Morphometry using deformation tensors*, MICCAI (2007).
- [18] Leporé N et al., *Fast 3D fluid registration of brain magnetic resonance Images*, SPIE (2008).
- [19] Miller MI, *Computational anatomy: shape, growth and atrophy comparison via diffeomorphisms*, Neuroimage 23, Suppl 1, (2004) 19–33.
- [20] Nichols TE, Holmes AP, *Non-parametric permutation tests for functional neuroimaging: a primer with examples*, Hum. Brain Map. 15, (2001) 1–25.
- [21] Pennec X et al., *Riemannian elasticity: A statistical regularization framework for non-linear registration*, MICCAI (2005).
- [22] Studholme C et al., *Deformation tensor morphometry of semantic dementia with quantitative validation*, Neuroimage 21, (2004) 1387–1398.
- [23] Thompson PM et al., *Genetic influences on brain structure*, Nat. Neurosc. 4, (2001) 1253–1258.
- [24] Thompson PM et al., *Mapping genetic influences on human brain structure*, Ann. of Med. 34, (2002) 523–536.